ELSEVIER

Journal of Nuclear Materials 255 (1998) 105–115

journal of nuclear materials

Hydrogen isotopes transport parameters in fusion reactor materials

E. Serra [a,*,1], G. Benamati [b], O.V. Ogorodnikova [c,2]

[a] *Dipartimento di Energetica, Politecnico di Torino, C.so Duca degli Abruzzi 24, 10129 Torino, Italy*
[b] *ENEA Fusion Division, CR Brasimone, 40032 Camungnano, Bologna, Italy*
[c] *Moscow State Engineering Physics Institute, Moscow 115409, Russia*

Received 12 January 1998; accepted 16 February 1998

Abstract

This work presents a review of hydrogen isotopes–materials interactions in various materials of interest for fusion reactors. The relevant parameters cover mainly diffusivity, solubility, trap concentration and energy difference between trap and solution sites. The list of materials includes the martensitic steels (MANET, Batman and F82H-mod.), beryllium, aluminium, beryllium oxide, aluminium oxide, copper, tungsten and molybdenum. Some experimental work on the parameters that describe the surface effects is also mentioned.

1. Introduction

An extensive research programme has been undertaken on hydrogen–material systems in recent years, yielding many interesting results of both commercial and scientific nature. The technological interest has its basis in the study of hydrogen embrittlement in many industrial applications such as petrochemical plants, chemical reactors, pipe lines and so on. Further, in nuclear plants, the safety aspects connected with the presence of hydrogen isotopes (tritium) in the existing fission reactors and in the future fusion plants require special attention to the evaluation of the hydrogen isotopes–material interaction parameters. In thermonuclear fusion devices, the fuel is a high temperature deuterium–tritium plasma. Because of their high energy, deuterium and tritium atoms and ions can enter the confinement structures by implantation. It is important to predict and control the deuterium and tritium Inventory in, Permeation through and Recycling from (IPR) the reactor walls, where, in general, inventory and permeation should be minimised. Numerical codes have been developed to simulate possible fusion reactor operation and to predict and control inventory, permeation and recycling of deuterium and tritium. Input data for these codes are details of the particle flux on the wall, wall material properties, and parameters describing the interaction of hydrogen isotopes with the materials. In addition, tritium produced in the breeder blanket by neutrons interacting with lithium nuclei can enter the metal structures, and can be lost by permeation to the outside. Tritium IPR in metallic components should therefore be kept under close control throughout the fusion reactor lifetime, bearing in mind the risk of accidents and the need for maintenance.

The purposes of the present review are to analyse the existing data for the hydrogen isotopes diffusivity, solubility, trap concentration and energy difference between trap and solution sites for the materials envisaged as structural and/or armour materials in the first wall and blanket of the next fusion reactors.

2. Basic theory

The hydrogen concentration of species i, c_i, in a wall of thickness d at depth x and time t is composed of a solute concentration c_{si} and trapping concentration c_{ti}:

$$c_i(x,t) = c_{si}(x,t) + c_{ti}(x,t). \quad (1)$$

* Corresponding author. Tel.: +39-534 801 225; fax: +39-534 801 463; e-mail: emanuele@netbra.brasimone.enea.it.
[1] ENEA scientific visitors.
[2] ENEA scientific visitors

0022-3115/98/$19.00
PII: S0022-3115(98)00038-5

The value of i indicates protium, deuterium or tritium. c_s for one of the hydrogen isotopes is given by the diffusion equation

$$\frac{\partial c_s}{\partial t} = -\frac{\partial J_s}{\partial t} + G(x,t) - \frac{\partial c_t}{\partial t} \tag{2}$$

where J_s is the local diffusive flux and G is the source term. Trapping is a process that delays the flow of hydrogen in a solid via the capture and release of hydrogen atoms by sites other than the ordinary solution ones. The parameters that characterise the trapping phenomenon are the number of trap sites N_t and their average energies E_t. The equation for J_s

$$J_s = -D\left(\frac{\partial c_s}{\partial x} + c_s \frac{Q}{RT^2}\frac{\partial T}{\partial x}\right) \tag{3}$$

contains two hydrogen–material interaction parameters, the diffusivity D which describes the hydrogen transport in a concentration gradient and the heat of transport Q, which describes the hydrogen transport in a temperature gradient. The boundary conditions at the inner and outer surface of the wall at $x = 0$ and $x = d$ are

$$J_s\left(x = \left\{\begin{matrix}0\\ d\end{matrix}\right\}, t\right) = k_1 p - k_2 c_s^2\left(x = \left\{\begin{matrix}0\\ d\end{matrix}\right\}, t\right), \tag{4}$$

where k_1 and k_2 are the adsorption and release surface constants, respectively, and p is the hydrogen gas pressure. Between Sieverts' constant or solubility at unit pressure K_s and the surface constants k_1, k_2 exists in the relation $k_1 = k_2 K_s^2$.

Summarising, it is possible to see that numerical codes for the calculation of recycling, inventory and permeation of hydrogen in fusion reactor walls need the hydrogen–material interaction properties: D, K_s, Q, k_1 N_t and E_t. Finally, in this work, the units for the diffusivity D and Sieverts' constant K_s are $m^2\ s^{-1}$ and mol m^{-3} $Pa^{-1/2}$, respectively. D and K_s are expressed as Arrhenius' equations:

$$D = D_0 \exp(-E_m/RT) \tag{5}$$

$$K_s = K_{s0} \exp(-Q_s/RT) \tag{6}$$

($R = 8.314$ J K^{-1} mol^{-1}). The hydrogen solubility is given by Sieverts' law: $S = K_s\sqrt{p}$ (p = hydrogen pressure (Pa)) and the permeability P (mol m^{-1} s^{-1} $Pa^{-1/2}$) is given by Richardson's law: $P = DK_s$.

3. Data for MANET, Batman and F82H-mod. martensitic steels

The martensitic steel DIN 1.4914 (MArtensitic for NET, MANET) is a Nb bearing steel, which has a better swelling

Table 1
Chemical composition (measured) of MANET II, F82H-mod. and Batman (wt.%)

	MANET II[a] (Net-heat No. 50803)	F82H-mod. Heat No. 9741	BATMAN Cast No. Cbis
C	0.11	0.09	0.125
Cr	10.3	7.88	8.67
Ni	0.65	0.02	0.021
Mo	0.58	< 0.01	0.0123
V	0.19	0.16	0.2
Nb	0.14	< 0.01	0.002
Si	0.18	0.11	0.025
Mn	0.85	0.16	0.52
S	0.004	0.002	0.0018
P	0.005	0.002	0.006
B	0.0072	0.0002	0.0064
N	0.03	0.005	0.0057
Co	0.006	< 0.01	0.01
Ta	–	0.02	–
Al	0.012	0.01	0.0084
Cu	0.01	< 0.01	0.0048
W	–	2	1.43
Ti	–	0.01	0.07
Zr	0.014	–	–
Zn	0.001	–	–
Sb	0.0004	–	–
Sn	–	–	0.0021
Pb	–	–	0.005
As	0.01	–	–
Fe	Balance	Balance	Balance

[a]MANET II is a further development of MANET.

resistance, lower sensitivity to helium embrittlement and more suitable thermophysical properties than the austenitic stainless steel AISI 316L. For these reasons, MANET had been the candidate material for the first wall and structure for the demonstration fusion reactor DEMO for several years. Since 1995, reduced activation martensitic (RAM) steels belonging to the 7–10% Cr martensitic steel class that have undergone some modification in order to achieve better low-activation characteristics compared with those of MANET have been assumed as reference. The RAM steels modified F82H (F82H-mod.) and Batman (Japanese and Italian, respectively) are still undergoing development and characterisation from the point of view of their mechanical and physical properties. In Table 1, the compositions of MANET, Batman and F82H-mod. martensitic steels are given. The hydrogen diffusivities and Sieverts' constant values are presented in Table 2. These data were obtained by gas permeation experiments, except the data of Ref. [5] that were obtained by a gas evolution method.

The hydrogen and deuterium diffusivities in MANET are shown in Fig. 1. The data spread is not particularly significant. One reason that probably influenced the results were the surface conditions of the specimens used during the measurements. Only in Refs. [6,7], the surface of samples were kept under control for the presence of oxide layers. In Refs. [6,7], before the membranes were inserted into the permeation equipment, both sides were mechanically polished. Thus, only oxide layers resulting from exposure to air at room temperature should be present in these experiments. It is known that the diffusion coefficient can decrease in the presence of impurities on the surface of the metal. Therefore, the reduction of the diffusion coefficient in Ref. [5] compared to that in Ref. [6] can be explained by the presence of contamination on the surface of samples.

A comparison of the deuterium diffusion coefficients for different martensitic steels, Batman, MANET and F82H-mod., is given in Fig. 2. As expected, there are only few differences in the deuterium diffusion coefficient among these metals because they belong to the same class of martensitic steels.

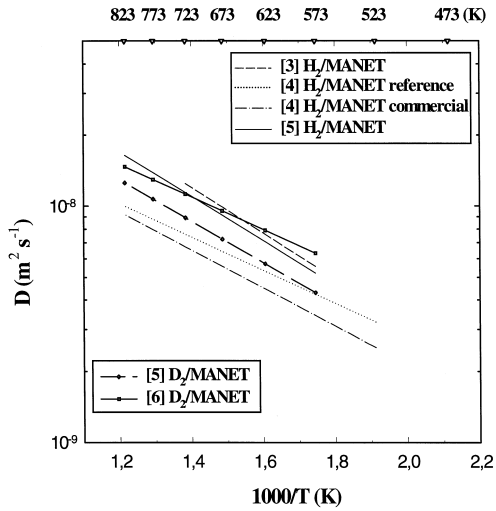

Fig. 1. Temperature dependence of hydrogen and deuterium diffusivity in MANET [3–6].

The Arrhenius expressions for the deuterium k_1 and k_2 surface constants of bare MANET were measured in Ref. [8]:

$$k_1 = 5.56 \times 10^{-7} \exp(-19093/RT)\ \mathrm{mol\,m^{-2}\,s^{-1}\,Pa^{-1}} \quad (7)$$

$$k_2 = 7.63 \times 10^{-6} \exp(-34247/RT)\ \mathrm{mol^{-1}\,m^{4}\,s^{-1}} \quad (8)$$

The trapping process in MANET, F82H-mod. and Batman is very pronounced in the low temperature range up to 523 K. It is evident from the results shown in Fig. 2 that the measured diffusion coefficients for all martensitic

Table 2
Arrhenius constants of hydrogen and deuterium diffusivities and Sieverts' constant values in the low activation martensitic steels

Material	Diffusivity		Sieverts' constant		Temperature	Reference
	D_0 (m^2/s)	E_m (kJ/mol)	K_{s0} ($mol/m^3\sqrt{Pa}$)	Q_s (kJ/mol)	T (K)	
H_2-α-Fe	3.87×10^{-8}	4.5	0.51	27	573–873	[1]
H_2-α-Fe	6.2×10^{-8}	10.5	1.7	23		[2]
H_2-F82H-mod.	9.2×10^{-8}	13.7	0.63	27.4	473–723	[3]
H_2-MANET reference	7.17×10^{-8}	13.49	0.409	29.62	523–873	[4]
H_2-MANET commercial	8.82×10^{-8}	15.47	0.373	26.89	523–873	[4]
H_2-MANET II[a]	2.28×10^{-7}	18	0.396	28.4	573–873	[5]
H_2-MANET II	2.7×10^{-7}	18.5	0.52	30	573–723	[3]
D_2-MANET II[a]	1.46×10^{-7}	16.8	0.658	32	573–873	[5]
D_2-MANET II	1.01×10^{-7}	13.2	0.27	26.7	573–723	[6]
D_2-Batman	1.9×10^{-7}	15.2	0.198	24.7	573–723	[6]
D_2-F82H-mod.	1.07×10^{-7}	13.9	0.377	26.8	573–723	[6]
H_2-F82H-mod.	1.8×10^{-7}	14.09	0.3	25.83	573–723	[7]

[a]Gas evolution method.

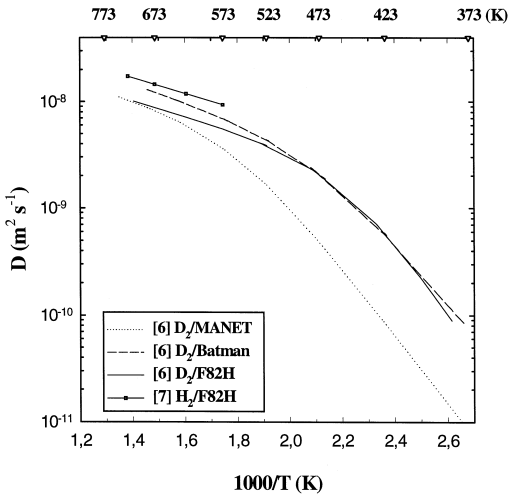

Fig. 2. Temperature dependence of hydrogen and deuterium diffusivity in different martensitic steels [6,7].

steels, in the lower part of the temperature interval (373–523 K), drop sharply below the lines representing the data at higher temperatures (633–743 K). The trapping parameters such as the numbers of trap sites N_t (sites/m^3) and their average energies E_t (kJ/mol) in martensitic steels, were determined in Refs. [1,9,6,10,11]. The data of the trap concentration N_t and trapping energy E_t in iron and martensitic steels are given in Table 3. Some values for the trapping energy in various types of traps in ferritic steels are presented in Table 4. It is worth noting that substitutional elements that are located on the right of iron in the periodic table, i.e., Ni, should repel hydrogen when present in the solid solution, while elements on the left of iron should trap hydrogen. This is confirmed in the literature [14], which indicates that substitutional Ni atoms are a repulsive trap in an iron lattice. Single vacancies should only exist in significant quantities in irradiated materials. A number of authors, e.g., Ref. [22], has suggested that lattice defects that have a coherent interface with the surrounding matrix such as dislocations and fine precipitates in the early stages of formation, have a lower trapping energy than, for example, fully coarsened second phase particles that have incoherent boundaries with the

Table 4
Trapping energies of hydrogen in ferritic steels and iron alloys

Type of trap	Trapping energy (kJ/mol)	Reference
Single vacancy	50	[12]
	46.4 and 78.3	[13]
Atomic traps		
Cr	26.1	[14]
	9.6	[15]
V	15.4	[15]
Ti	26.1	[15]
Nb	15.4	[15]
Zr	24–36	[16]
Y	130	[17]
Ni	8	[15]
Substitutional Ni	−11.6	[14]
Ce	15.4	[15]
O	71	[15]
La	94.5	[15]
Ta	94.5	[15]
Nd	129	[15]
Mo	27.1	[14]
C	3.3	[18]
N	12.5	[18]
Grain boundaries	59	[19]
	32	[20]
Second-phase particles (surfaces)		
AlN	65	[21]
TiC	94	[22]
	80–90	[15]
ε-carbide (Fe_3C)	65	[23]
	87	[24]
MnS	72	[23]
	80	[25]
Dislocation	25	[26]

Table 3
Trapping parameters of iron and martensitic steels

Material	E_t (kJ/mol)	N_t (sites/m^3)	Method[a]	Temperature (K)	Reference
α-Fe	69	4.2×10^{23}	GPPT	373–873	[1]
MANET II AR	22.425	3.4×10^{28}	EM	298	[9]
MANET II HT	22.89	3.6×10^{28}	EM	298	[9]
Batman	43.175	8.6×10^{24}	GPPT	373–723	[6]
F82H-mod.	55.938	1.6×10^{23}	GPPT	373–723	[6]
MANET II	48.5	1.5×10^{25}	GPPT	373–723	[6]
MANET II	39.5	1.5×10^{25}	DT	310–450	[10]
MANET II	61.3	6.2×10^{23}	GPPT	467–728	[11]

[a]GPPT = Gas-phase permeation technique.
DT = Desorption test.
EM = Electrochemical method.

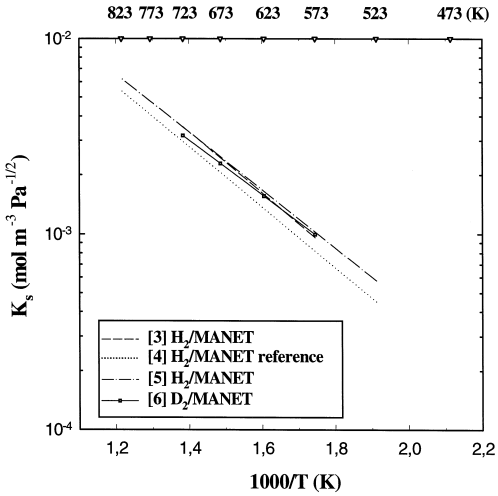

Fig. 3. Temperature dependence of hydrogen and deuterium Sieverts' constant in MANET [3–6].

metal lattice. It is useful to compare the data obtained for MANET using a gas-phase permeation technique method [6] in the temperature range 373–723 K and the data obtained using Devanathan's electrochemical technique [9] at 298 K. The electrochemical method gives a lower value of the trapping energy E_t, but a higher value of the concentration of traps N_t in comparison to the gas-phase permeation method. In Ref. [9], traps such as fully coarsened particles were 'irreversible traps' because of their depths, i.e., the detrapping rate was too low to allow equilibrium between the trapped and non-trapped populations to occur during a measurement. The gas-phase permeation method allowed the characterisation of these kinds of traps. It seems that in MANET, F82H-mod. and Batman trapping is more likely to be associated with the lath boundaries (martensitic laths) with fine coherent Fe_3C precipitates and with dislocations.

The hydrogen [6] and deuterium [7] diffusivities for F82H-mod. are also shown in Fig. 2. The factor difference between the diffusivities of deuterium and hydrogen over the entire temperature range through F82H-mod., is a factor 1.6, compared to the expected value of $\sqrt{2}$ for the classical diffusion theory. The average factor difference between the diffusivities of deuterium and hydrogen for MANET was found to be 1.3 [5] (see Fig. 1).

The hydrogen and deuterium Sieverts' constants for MANET are shown in Fig. 3. The hydrogen and deuterium Sieverts' constants for different martensitic steels, Batman, MANET and F82H-mod., are shown in Fig. 4. There is very good agreement among these data. As expected, there is no isotopic effect on the solubility in MANET and F82H-mod. steels.

Hydrogen permeabilities ($P = DK_s$) through MANET [3–5] are shown in Fig. 5. The comparison of deuterium permeabilities through MANET and Batman martensitic steels in the temperature range 373–723 K is given in Fig. 6 [6]. In this figure are shown the permeabilities in the F82H-mod. steel of both hydrogen [7] and deuterium [6] that illustrates again the isotope effect. The activation energies for the permeation of the two isotopes differ by only 3%, which is not significant. The factor difference between the permeabilities of deuterium and hydrogen over the entire temperature range 373–723 K through F82H-mod. is again a factor 1.6, compared to the expected value of $\sqrt{2}$ for the classical theory. In Ref. [4], the average

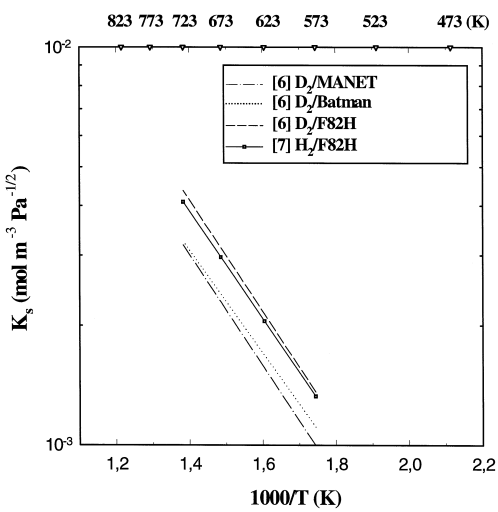

Fig. 4. Temperature dependence of hydrogen and deuterium Sieverts' constant in different martensitic steels [6,7].

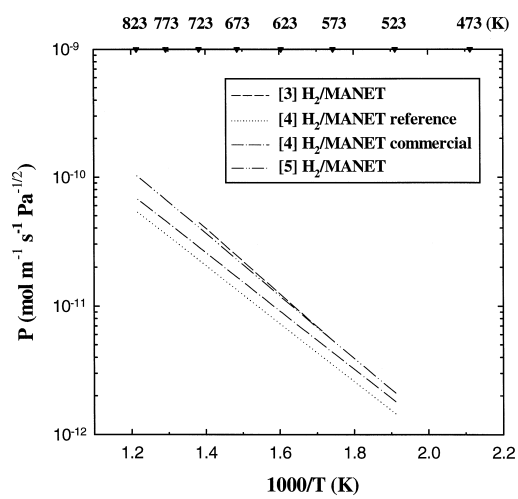

Fig. 5. Arrhenius plot of hydrogen permeabilities for MANET [3–5].

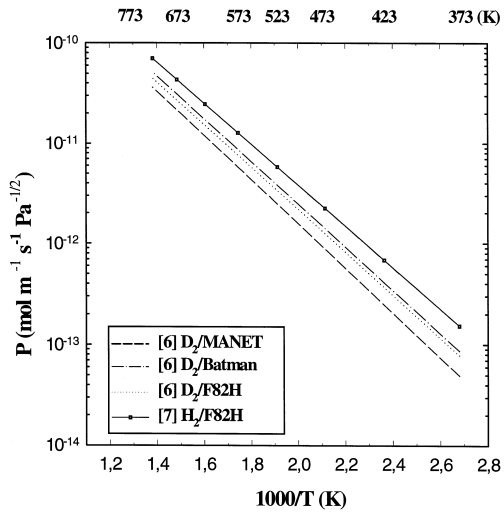

Fig. 6. Arrhenius plot of hydrogen and deuterium permeabilities for MANET, F82H and Batman steel [6,7].

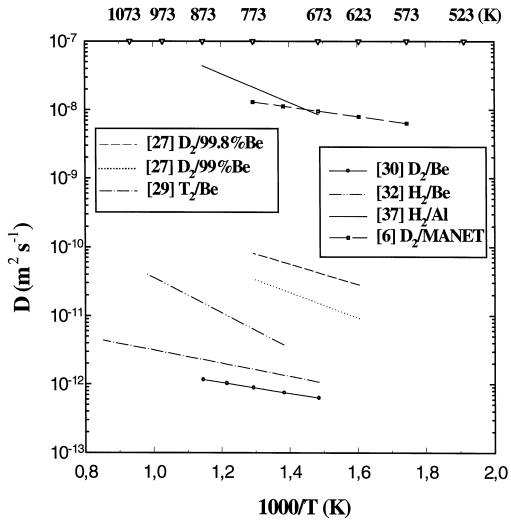

Fig. 7. Temperature dependence of hydrogen isotopes diffusivity in beryllium [27,29,30,32], aluminium [37] and MANET [6].

factor difference between the permeabilities of deuterium and hydrogen for MANET was found to be 1.4

4. Data for beryllium

Beryllium is one of the candidate plasma-facing materials for fusion reactors such as ITER. Beryllium has been proposed because of its low Z and good thermal characteristics, and it can getter oxygen in a plasma environment. Data of the solubility and diffusivity of hydrogen isotopes for Be are summarised in Table 5. In Fig. 7, hydrogen isotope diffusivities for Be are shown. The spread of the diffusion coefficient for Be is very large. The purity of the beryllium samples used in these experiments strongly affected the results. The influence of surface conditions, especially surface oxides, in the measurements of diffusivity in beryllium is very strong. In Ref. [27], the authors used a deuterium gas-driven permeation technique in the temperature range 620–775 K and eliminated the effect of surface oxide layers in Be samples, employing a multi-layer permeation theory. The diffusivity of BeO was taken from Ref. [35] (see Section 6). It was shown that the contribu-

Table 5
Data of diffusivity and solubility of hydrogen isotopes for beryllium and beryllium oxide, aluminium and aluminium oxide

Material	Diffusivity		Sieverts' constant		T (K)	Reference
	D_0 (m^2/s)	E_m (kJ/mol)	K_{s0} (mol/m$^3\sqrt{Pa}$)	Q_s (kJ/mol)		
D_2–99.8%Be	6.7×10^{-9}	28.4			620–775	[27]
D_2–99.0%Be	8×10^{-9}	35.1			620–775	[27]
T_2–99.8-98.5%Be			5.9×10^{3}	96.5	713–783	[28]
T_2–Be	3×10^{-11}	18.47	1.964×10^{-3}	-1.82×10^{-3}	673–1173	[29]
D_2–Be	9×10^{-12}	14.9			673-873	[30]
T_2–Be			1.9×10^{-2}	16.7	673–1473	[31]
H_2–Be	1.3×10^{-8}	49	1.1×10^{2}	25	740–1000	[32]
H_2–Be			2.25×10^{-3}	−1.819	523–1123	[33]
D_2–BeO[a]	2×10^{-5}	202.6	8×10^{-7}	77.2	773	[34]
T_2–single-crystal BeO[b]	1.1×10^{-6}	220			923–1473	[35]
T_2–sintered BeO[b]	7×10^{-5}	203			773–1223	[35]
H_2–Al	2.1×10^{-5}	45.6	8.19	81.2	723–873	[36]
H_2–Al	1.1×10^{-5}	40.1	0.5	63.2	623–873	[37]
T_2–single-crystal Al_2O_3[b]	3.3×10^{-4}	239			873–1273	[35]
T_2–sintered Al_2O_3[b]	7.35×10^{-6}	183.3			873–1173	[35]
D_2–Al_2O_3			5.9	75.7	973–1573	[38]

[a] Thermodesorption method (thermal adsorption and desorption experiments).
[b] The time rate of tritium release during post-irradiation heating method.

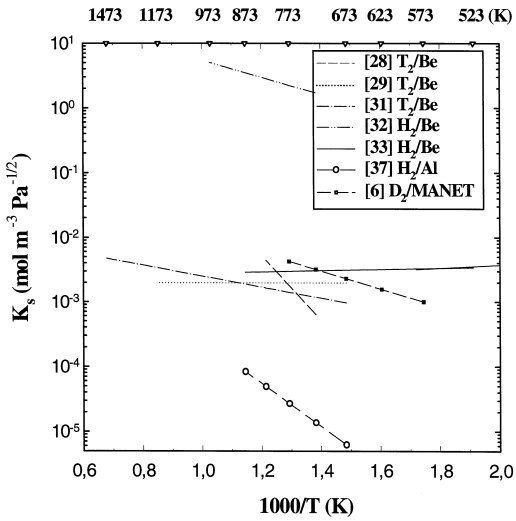

Fig. 8. Temperature dependence of hydrogen isotopes Sieverts' constants for beryllium [28,29,31,33], aluminium [37] and MANET [6].

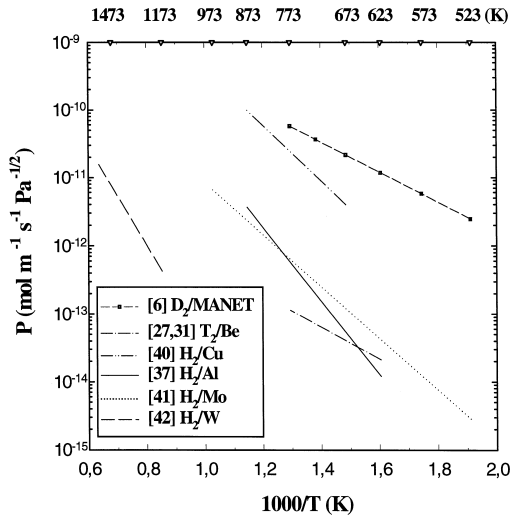

Fig. 9. Arrhenius plot of hydrogen isotopes permeabilities through MANET [6], beryllium [27,31], aluminium [37], copper [40], molybdenum [41] and tungsten [42].

tion of a BeO layer to the permeation can be significant. The influence of surface oxides is quite difficult to predict in the desorption and permeation experiments. The presence of a BeO layer on the surface of the sample decreases the diffusion coefficient. Also in Ref. [29], using a multilayer penetration theory (diffusivity of BeO was again taken from Ref. [35]), the deuterium diffusivity of beryllium was determined. The results are in agreement with the results of Ref. [29], but in disagreement with the results of Ref. [27]. A possible explanation of this discrepancy might be connected with the different purity of Be and the different sample preparation (a thin-rolled foil significantly differs from a wafer cut of a rod). In Ref. [39], using a gas-driven permeation technique, the authors reported a large variation in permeability depending on the beryllium grain size. Thus, the diffusion behaviour is strongly dependent on the purity and preparation of the tested material: the activation energy of diffusion E_m for beryllium varies from 14.9 kJ/mol [30] to 49 kJ/mol [32].

In Fig. 8, Sieverts' constants for hydrogen isotopes in Be are shown. The spread also for Sieverts' constant is significant. The solubility data obtained using the desorption technique again strongly depend on the surface conditions of the samples. In a charging/desorption experiment [29], it was found that the tritium Sieverts' constant for beryllium was 1.964×10^{-3} (mol m^{-3} $Pa^{-1/2}$) and also independent of temperature. In this work, the achievement of saturation was not proved. In Ref. [28], the authors reported a heat of solution for Be of 96.5 kJ/mol. Therefore, the activation energy of solution for Be can vary from about 0 to 100 kJ/mol.

The most reliable data for Be are presented in Table 6. In Fig. 9, the tritium permeability ($P = DK_s$) for pure beryllium is shown. From this figure, it is possible to see that the tritium permeabilities through Be are about three orders of magnitude lower than those through MANET steel, so that Be can reduce sensibly the permeation flux through the first wall of fusion reactors.

5. Data for aluminium

Aluminium is a candidate material in order to produce tritium permeation barriers (TPB) by formation of aluminium-rich coatings which form Al_2O_3 at their surfaces, in the blanket of the reactor. It is used because it has a high heat of solution $Q_s = 63.2$ kJ/mol [37] and activation energy of diffusion $E_m = 40.1$ kJ/mol [37] compared to

Table 6
The most reliable data of diffusivities and Sieverts' constants of hydrogen isotopes in beryllium and aluminium

Material	Diffusivity		Solubility		Reference
	D_0 (m^2/s)	E_m (kJ/mol)	K_{s0} (mol/$m^3\sqrt{Pa}$)	Q_s (kJ/mol)	
D_2–Be	6.7×10^{-9}	28.4			[27]
T_2–Be			1.8×10^{-2}	16.4	[31]
H_2–Al	1.1×10^{-5}	40.1	0.5	63.2	[37]

those of MANET. Moreover (see Section 6), the hydrogen permeability in aluminium oxide is many orders of magnitude lower compared to that in the martensitic steels. Data of the solubility and diffusivity of hydrogen isotopes in bare Al are presented in Table 5. The most reliable data for Al are presented in Table 6. In Fig. 9, the hydrogen permeability ($P = DK_s$) for aluminium is shown. At low temperature, Al has a hydrogen permeation flux of about six orders of magnitude lower than that of a bare martensitic steel.

In Refs. [43,44], an estimate of the trapping parameters for Al is reported. Hydrogen trapping in aluminium shows a number of traps N_t of about 3×10^{27} sites/m^3 and an activation energy of trapping E_t between 130 and 193 kJ/mol. It can be noted that the trapping parameters E_t and N_t for Al are higher than those for martensitic steels (see Table 2). Hydrogen trapped with an energy $E_t = 100$ kJ/mol is usually released from these traps at about 400 K if it is trapped with an energy $E_t = 200$ kJ/mol it is released at about 800 K, and so on. Therefore, while the trapping phenomenon in the martensitic steels decreases rapidly at temperatures above 400 K ($E_t = 40$–60 kJ/mol), hydrogen is strongly trapped in Al at about 600 K ($E_t = 150$ kJ/mol).

6. Data for aluminium oxide and beryllium oxide

Two observations can be made regarding permeation properties of hydrogen in ceramic materials: (1) the permeation rate is much less than that in metals; (2) the activation energies are very high, 3 to 10 times higher than those of metals. This suggests that a strong interaction exists between the diffusing hydrogen isotopes and the host lattice. For these reasons, alumina is investigated as TPB.

Hydrogen isotopes diffusivities in Al_2O_3 and BeO were reported in Refs. [34,35]. Measured diffusivities in Al_2O_3 and BeO are many orders of magnitude lower compared to diffusion coefficients for bare Be and Al (Table 5). In general, the solubility data for ceramics are confusing. The reasons are: (1) the solubility is low and permeation rate are extremely low, requiring long equilibration times; (2) impurity effects become very important in trapping hydrogen; (3) different physical states of the material, including the crystalline form, show different characteristics. The most reliable data for alumina are reported in Ref. [38].

The permeability through aluminium oxide and beryllium oxide is much less than through pure aluminium and pure beryllium. A comparison of hydrogen permeabilities for beryllium metal and beryllium oxide is shown in Fig. 10. It is worth noting that the Arrhenius plots of the permeabilities for Be and BeO do not follow the tendency known for other metals: increasing the temperature, the permeability of all metals tends to the same value and it does not depend on the temperature any more. These peculiarities let us suppose that some mistakes affect the experimental data for Be.

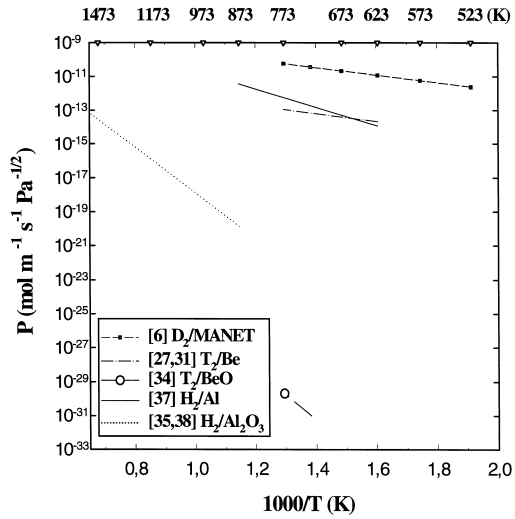

Fig. 10. Arrhenius plot of hydrogen isotopes permeabilities through steels [6], beryllium [27,31], beryllium oxide [34] aluminium [37] and alumina [35,38].

7. Data for copper

Copper metal has a fcc lattice and does not form a hydride by direct reaction with hydrogen. The diffusivity and the solubility of hydrogen in copper have been determined by various investigators over an extended period of time. The difficulties caused by the presence of oxygen in obtaining good hydrogen diffusion data have long been recognised [45,46]. The most reliable data of hydrogen diffusivity and solubility obtained with high purity samples of copper are given in Ref. [40] (Table 7) and are shown in Fig. 9. In Refs. [40,47], it was observed that the isotopic ratios are less than those predicted by the inverse mass relationships $(m_D/m_H)^{1/2}$ and $(m_T/m_H)^{1/2}$. The authors [40,47] theoretically analysed their observed isotopic ratios. In Ref. [47], the authors conclude that a quantum mechanical harmonic model is sufficient to describe the isotope effect for diffusion in copper.

Pure aluminium has a lower permeability than pure copper (see Fig. 9). Nevertheless, for copper a hydrogen trapping behaviour was found similar to that of aluminium [58].

8. Data for molybdenum and tungsten

Because of their refractory nature and good thermal properties, Mo and W are considered to be alternatives to graphite as plasma-facing materials, especially for a diver-

Table 7
Data of diffusivity and solubility of hydrogen isotopes for copper, molybdenum and tungsten

Material	D_0 (m^2/s)	E_m (kJ/mol)	K_{s0} ($mol/m^3\sqrt{Pa}$)	Q_s (kJ/mol)	T (K)	p (Pa)	Reference
H_2–Cu	1.15×10^{-6}	40.8			703–913	$1–9\times10^4$	[40]
H_2–Cu			4.5	38	703–908	$1–9\times10^4$	[40]
D_2–Cu	6.2×10^{-7}	37.8			703–913	$1–9\times10^4$	[40]
D_2–Cu			5.3	40	703–908	$1–9\times10^4$	[40]
H_2–Cu	1.13×10^{-6}	38.9			723–1198		[47]
D_2–Cu	7.3×10^{-7}	36.8			723–1073		[47]
T_2–Cu	6.12×10^{-7}	36.5			723–1073		[47]
H_2–Cu			0.7	38.4	1007–1343	$9\times10^3–10^5$	[48]
H_2–Mo	4.8×10^{-7}	37.7			1123–2023		[49]
H_2–Mo			0.72	52.2	1178–1794	10^5	[50]
H_2–Mo	3.5×10^{-7}	58.6			523–2023		[51,52]
H_2–Mo	2×10^{-6}	61.5	0.18	28.5	623–1773		[53]
H_2–Mo			0.36	39.8	873–1473	10^5	[54]
H_2–Mo	1×10^{-6}	58.6	0.72	52.2	1173–1773		[37]
H_2–Mo	4×10^{-8}	22.3	3.3	37.5	500–1100	$1–10^5$	[55]
H_2–Mo	$\approx 6\times10^{-8}$	16.3	≈ 1	54.7	723–1173	10^5	[56]
H_2–Mo Single cryst.	2×10^{-4}	75	$7\cdot10^{-4}$	2.9	673–1473	$10^2–3\times10^4$	[57]
H_2–Mo Polycryst.	2×10^{-4}	75	$1.8\cdot10^{-3}$	6.3	673–1473	$10^2–3\times10^4$	[57]
H_2–W	4.1×10^{-7}	37.7	1.47	100.4	1173–2073	7×10^4	[42]
H_2–W	6×10^{-4}	103.4	$1.2\cdot10^{-4}$	2.9	673–1473	$10^2–3\times10^4$	[57]

tor plate operated in the low edge temperature (≈ 10 eV)/high recycling plasma mode. Both Mo and W are refractory metals having a bcc lattice, and do not form binary hydrides with hydrogen [59].

Hydrogen diffusion data for Mo are not in agreement (see Table 7 and Fig. 11). The selection of a recommended diffusion coefficient is difficult. The calculated hydrogen diffusivities of Ref. [49], using the permeation results of Ref. [60] and the solubility data of Ref. [50], are recommended to be most representative. Very few determinations of the hydrogen solubility in molybdenum exist, and those that have been reported are of questionable validity because there is no agreement among different investigations (see Table 7 and Fig. 12). The solubility data of Ref. [50] are recommended because these data were obtained with single crystal samples of very high purity. Extrapolation of these solubility data [50] to lower loading pressures ($\ll 10^5$ Pa) is questionable because the solubility in Mo is expected to show an anomalous behaviour at low pressures

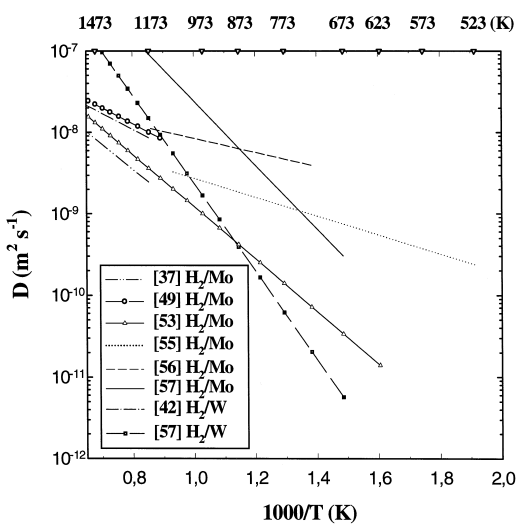

Fig. 11. Temperature dependence of hydrogen diffusivity for molybdenum [37,49,53,55–57] and tungsten [42,57].

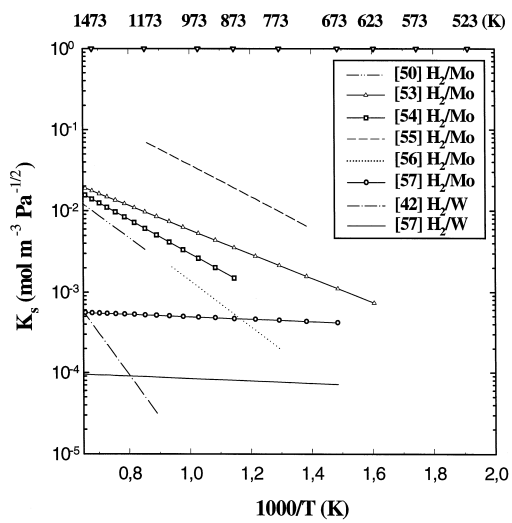

Fig. 12. Temperature dependence of hydrogen Sieverts constant for molybdenum [50,53–57] and tungsten [42,57].

and relatively high temperatures, as reported in Refs. [60,53].

The best available data for diffusion and solution of hydrogen in tungsten are those obtained in Ref. [42] (between 1173 and 2073 K) (see Table 7 and Figs. 11 and 12). As for Mo, the observed solubility at low pressure is considerably larger than that predicted by extrapolation of data obtained at a high loading pressure.

The data of hydrogen diffusivity and Sieverts' constant for Mo and W are presented in Table 7 and are shown in Figs. 11 and 12, respectively.

Since the oxides of Mo and W are volatile, surface oxides can be easily removed by high-temperature annealing in vacuum. It was found that the presence of water vapour, included in the hydrogen gas as main impurity, does not influence the hydrogen permeation in Mo [61]. Therefore, it seems difficult to use, for Mo, an oxide layer as a permeation barrier. Carbon and sulphur, the main impurities, are difficult to remove because of the high-temperature solubility of the metal carbide and sulphide. However, their impact on hydrogen transport properties is unknown.

In Fig. 9, hydrogen permeabilities ($P = DK_s$) in tungsten [42] and molybdenum [41] are shown, which are lower compared to those for martensitic steels. However, the hydrogen permeability in Mo [41] is about three orders of magnitude higher than that in W [42] at 773 K, and the activation energy for permeation is two times lower in Mo [41] (72.8 kJ/mol) than that in W [42] (138.1 kJ/mol).

From deuterium permeation data analysis in the range 610–823 K, the authors [62] found that trapping affects significantly the deuterium transport in W, and it was estimated that trap energies vary from 130 to 150 kJ/mol, and trap concentrations from 6×10^{23} to 4×10^{24} sites/m^3 for unannealed and annealed tungsten, respectively. In the temperature range 673–1473 K, the trapping phenomenon can explain the difference for both diffusivity and solubility data of hydrogen in W between Ref. [42] (extrapolated data) and Ref. [57].

Very few data exist for deuterium and tritium transport parameters in Mo and W.

9. Conclusions

The present work summarises the existing data of hydrogen isotopes transport and inventory parameters for several materials (metals and ceramics) of potential interest in fusion devices. As far as martensitic steels of interest for the DEMO reactor are concerned, the trapping phenomenon and surface effects are presented and discussed in addition to the diffusivity, solubility and permeability data. There are many factors that influence the measured hydrogen isotopes transport and inventory in materials. Regarding metals, the determination of these parameters depends on the surface contamination, the presence of natural oxide, grain boundaries, the trapping effect, the experimental method used, etc. On the base of the existing data it can be observed that there is a large spread in the database for beryllium, tungsten and molybdenum. Whereas it appears clear that a large and reliable database for the martensitic steels exists, the data for several armour materials such as Be and W are not sufficient.

The hydrogen isotopes permeabilities for the different materials proposed for fusion reactors are as follows: martensitic steels > Cu > Mo ≥ Be ≥ Al > W > Al_2O_3 > BeO. This means that materials such as beryllium or beryllium oxide, aluminium or aluminium oxide as well as tungsten can reduce the hydrogen permeation rate with respect to martensitic steels. It should be underlined that in most cases, the permeation rate through the ceramic layer such as Al_2O_3, used as TPB, seems to depend mainly on the integrity of the ceramic.

References

[1] K.S. Forcey, I. Iordanova, D.K. Ross, Mater. Sci. Technol. 6 (1990) 357.
[2] Y. Yamanishi, T. Tanabe, S. Imoto, Trans. Jpn. Inst. Met. 24 (N1) (1983) 49.
[3] C. Fazio, PhD thesis, Università di Padova, 1997.
[4] K.S. Forcey, D.K. Ross, J.C.B. Simpson, D.S. Evans, J. Nucl. Mater. 160 (1988) 117.
[5] A. Perujo, S. Alberici, J. Camposilvan, F. Reiter, Fusion Technol. 21 (1992) 800.
[6] E. Serra, A. Perujo, G. Benamati, J. Nucl. Mater. 245 (1997) 108.
[7] E. Serra, G. Benamati, J. Mater. Sci. Technol., to be published.
[8] E. Serra, A. Perujo, J. Nucl. Mater. 240 (1997) 215.
[9] G. Benamati, A. Donato, A. Solina, S. Lanza, J. Nucl. Mater. 212–215 (1994) 1401.
[10] R. Valentini, A. Solina, L. Tonelli, S. Lanza, G. Benamati, A. Donato, J. Nucl. Mater. 233–237 (1996) 1123.
[11] K.S. Forcey, I. Iordanova, M. Yaneva, J. Nucl. Mater. 240 (1997) 118.
[12] S.M. Myers, S.T. Picraux, R.E. Stroltz, J. Appl. Phys. 50 (1979) 5710.
[13] K.B. Kimand, S. Pyun, Arch. Eisenhuttenwers. 53 (1982) 397.
[14] A.I. Shirley, S.K. Hall, Scipta Metal. 17 (1983) 1003.
[15] G.M. Pressouyre, Metal. Trans. 10A (N10) (1979) 1571.
[16] H. Kronmüller, B. Hohler, R. Schreyer, K. Veter, Philos. Mag. B 37 (1978) 569.
[17] G.S. Ershov, A.A. Kasatkin, Izv. Akad. Nauk. SSSR Metally (1977) 82.
[18] J.J. Au, H.K. Birnbaum, Acta Metall. 26 (1978) 1105.
[19] J.P. Hirth, Metall. Trans. 11A (1980) 861.
[20] J.R. Scully, J.A. van den Avyle, M.J. Cieslak, A.D. Romig Jr., C.R. Hills, Metall. Trans. 22A (1991) 2429.
[21] H.H. Podgurski, R.A. Oriani, Metall. Trans. 3 (1972) 2055.
[22] G.M. Pressouyre, I.M. Bernstein, Metal. Trans. 9A (1978) 1571.

[23] J. Chene, J.O. Garcia, C.P. de Oliveira, M.A. Aucouturier, P. Lacombe, J. Microsc. Spectrosc. Electron. 4 (1979) 37.
[24] R. Gibala, D.S. De Miglio, Hydrogen Effects in Metals, in: I.M. Bernstein, A.W. Thompson (Eds.), TMS, Warrendale PA, 1981, p. 113.
[25] J.Y. Lee, J.L. Lee, W.Y. Choo, in: C.G. Interrante, G.M. Pressouyre (Eds.), Proc. First Intern. Conf. on Current Solutions to Hydrogen Problems in Steels, ASM, Washington DC, 1982, p. 423.
[26] C.A. Wert, Topics in Applied Physics, in: G. Alefeld, J. Völkl (Eds.), Hydrogen in Metals II, Vol. 29, 1978, p. 305.
[27] E. Abramov, M.P. Riehm, D.A. Thomson, W.W. Smeltzer, J. Nucl. Mater. 175 (1990) 90.
[28] W.A. Swansiger, J. Vac. Sci. Technol. A 4 (1986) 1216.
[29] P.M.S. Jones, R. Gibson, J. Nucl. Mater. 21 (1967) 353.
[30] I.L. Tazhibaeva, V.P. Shestakov, E.V. Chikhray, O.G. Romanenko, A.Kh. Klepikov, G.L. Saksaganskiy, Yu.G. Prokofiev, S.N. Mazaev, Proc. of the 18th Symposium on Fusion Technology, August 22–26, Karlsruhe, Germany, Fusion Technol., 1994, p. 427.
[31] V.I. Shapovalov, Ju. Dukel'skii, Russ. Metall. 5 (1988) 201.
[32] K. Kizu, T. Tanabe, Proc. 2nd Intern. Workshop on Tritium Effects in Plasma Facing Components, Nagoya, Japan, NIFS-PROC-19, 1994, p. 76.
[33] E. Fromm, H. Jehn, Alloy Phase Diagr. 5 (1984) 324.
[34] R.G. Macaulay-Newcombe, D.A. Thompson, J. Nucl. Mater. 212–215 (1994) 942.
[35] J.D. Flowler, D. Chandra, T.S. Elleman, A.W. Payne, K. Verghese, J. Am. Ceram. Soc. 60 (1977) 155.
[36] W. Eichenauer, A. Perbler, Z. Metallkd. 48 (1957) 373.
[37] E. Fromm, E. Gebhardt, Gase und Kohlenstoff in Metallen, Springer, Berlin, 1976.
[38] T.S. Elleman, R.A. Causey, D.R. Chari, P. Feng, R.M. Roberts, K. Verghese, L.R. Zumwalt, Tritium Diffusion in Nonmetallic Solids of Interest for Fusion Reactors, Annual Progress Report, ORO-4721-6 (1977).
[39] R.M. Al'tovskij, A.A. Eremin, L.F. Eremina, A.A. Izhvanov, V.N. Fadeev, M.I. Urazbaev, Izv. Akad. Nauk. SSSR Metally 3 (1981) 73.
[40] W. Eichenauer, A. Perbler, Z. Metallkd. 56 (1965) 287.
[41] J.W. Guthrie, L.C. Beavis, D.R. Begeal, W.G. Perkins, J. Nucl. Mater. 53 (1974) 313.
[42] R. Frauenfelder, J. Vac. Sci. Technol. 6 (1969) 388.
[43] K.L. Wilson, L.G. Haggmark, Thin Solid Films 63 (1960) 283.
[44] R. Daniels, J. Appl. Phys. 42 (1971) 417.
[45] W.R. Ham, J. Chem. Phys. 7 (1939) 903.
[46] E. Mattsson, F. Schückher, J. Inst. Met. 87 (1959) 241.
[47] L. Katz, M. Guinan, R.J. Borg, Phys. Rev. B 4 (1971) 330.
[48] F.G. Jones, R.D. Pehlke, Metall. Trans. 2 (1971) 2655.
[49] W.G. Perkins, J. Vac. Sci. Technol. 10 (1973) 543.
[50] W.A. Oates, R.B. McLellan, Scr. Metall. 6 (1972) 349.
[51] V.M. Katlinskiy, L.L. Kotlik, Russ. Metall. 2 (1978) 65.
[52] V.M. Katlinskiy, L.L. Kotlik, Engl. Transl. Izv. Akad. Nauk SSSR Metally 2 (1978) 80.
[53] R.E. Stickney, Diffusion and permeation of hydrogen isotopes in fusion reactors: A survey, the chemistry of fusion technology, in: D.M. Gruen (Ed.), Plenum, New York, 1972.
[54] T. Eguchi, S. Morozumi, Nippon Kinzoku Gakkaishi 38 (1974) 1019.
[55] T. Tanabe, T. Yamanishi, S. Imoto, J. Nucl. Mater. 191–194 (1992) 439.
[56] H. Katsura, T. Iwai, H. Ohno, J. Nucl. Mater. 115 (1983) 206.
[57] A.P. Zakarov, V.M. Sharapov, E.I. Evko, Soviet Mater. Sci. 9 (1973) 149.
[58] G.M. McCracken, J.H.C. Maple, Br. J. Appl. Phys. 18 (1967) 919.
[59] B. Siegel, G.G. Libowitz, The covalent Hydrides and Hydrides of the Groups V to VIII Transition Metals, in: W.M. Mueller, J.P. Blackledge, G.G. Libowitz (Eds.), Metal Hydrides, Academic Press, New York, 1968.
[60] R. Frauenfelder, J. Chem. Phys. 48 (1968) 3955.
[61] T. Tanabe, J. Nucl. Mater., in press.
[62] R.A. Anderl, D.F. Holland, G.R. Longhurst, R.J. Pawelko, C.L. Trybus, C.H. Sellers, Fusion Technol. 21 (1992) 745.